Post glacial readjustment, sea level variations, subsidence and erosion along the Italian coasts

P. Stocchi [a], L. Girometti [b], G. Spada [b,*], M. Anzidei [c]

[a] *DEOS, Faculty of Aerospace Engineering, Delft University of Technology, NL.*

[b] *Istituto di Fisica, Università di Urbino "Carlo Bo", Urbino, Italy.*

[c] *Istituto Nazionale di Geofisica e Vulcanologia, Rome, Italy.*

Abstract

Ongoing sea level variations and vertical land movements measured by tide gauges and continuous GPS stations along the Italian coasts stem from several factors acting on different spatiotemporal scales. Conversely to tectonics and anthropogenic effects, which are characterized by a heterogeneous signal, the adjustment of solid Earth and geoid to the melting of the late– Pleistocene ice sheets results in a smooth long–wavelength pattern of sea level variation and vertical deformation across the Mediterranean, mostly driven by the melt water load added to the basin. In this work we define upper and lower bounds of the effects of glacial isostatic adjustment (GIA) on current sea level variations and vertical ground movements along the coasts of Italy. For plausible mantle viscosity profiles we explore to what extent the spatial variability of observed rates may be attributed to delayed isostatic recovery of both solid Earth and geoid. In addition, we show that long–wavelength patterns of sea level change are tuned by the effects of GIA, and that coastal retreat in Italy is broadly correlated with **the expected** ongoing rates of post–glacial sea level variations.

---

* Corresponding author. Istituto di Fisica, Università di Urbino "Carlo Bo", Via Santa Chiara n. 27, 61029 Urbino (PU), Italy. Phone (Fax): +39 0722 303389 (99), email: giorgio.spada@gmail.com.

1 Introduction

Sea level is the offset between the surface of the geoid and that of the solid Earth at a given time [7/2] **(Farrell and Clark, 1976)**. When land glaciers melt, a corresponding variation of the ocean mass occurs globally (but not necessarily uniformly), thus resulting in a new sea level. The difference between new and the old sea level is referred to as sea level change, which results from the sum of three terms. The first (eustatic term) is the globally uniform variation that we would observe for a rigid, non gravitating Earth. The second and the third are due to geoid height variations and ground vertical deformations associated to ice and water loads, respectively. These latter terms have a complex spatiotemporal variability, being also dependent upon the delayed visco–elastic response of solid Earth (see e. g. Farrell and Clark 1976 and Spada and Stocchi 2006 for a review). Melting of Pleistocene ice sheets has resulted into a widespread variable sea level change, characterized by a long–wavelength pattern that reveals various regions sharing the same relative sea level curves as function of distance from the margins of former glaciers (Farrell and Clark, 1976; Clark and Lingle, 1979; Stocchi and Spada, 2007).

Middle to late Holocene geological indicators and coastal archaeological remains of Roman period ($\sim$ 2500 BP) show that, since the end of deglaciation, sea level rose to and never exceeded the present–day datum along the Italian coastlines (Pirazzoli, 1991; Lambeck et al., 2004a; Pirazzoli, 2005). The general shape of Holocene relative sea level curves expected in Italy is peculiar of enclosed basins, where water loading deforms sea floor and results in a significant and widespread subsidence (Lambeck and Purcell, 2005; Stocchi and Spada, 2007). Northern to central coasts of Italy are potentially the most affected by the process of isostatic adjustment of the former Alpine and Fennoscandian ice sheets (Stocchi et al., 2005), since ice unloading and the related forebulge collapse shapes the overall pattern of land subsidence to a distance of a few thousands km from the ice centers (Lambeck and Johnston, 1995).

The aim of this study is comparing model predictions with observations at sites where tide gauges and continuous GPS time–series are available, with the aim of establishing trade offs between various factors currently contributing to sea level change and subsidence (or uplift) in Italy. Assuming the ICE5G chronology for the former late–Pleistocene ice sheets (Peltier, 2004) and a suite of plausible mantle viscosity profiles, we solve the original form of the ”Sea Level Equation” (Farrell and Clark, 1976) to estimate current rates of **GIA–induced** sea level change and vertical deformation along the Italian region and to discuss their relationship with available instrumental observations (tide gauge and GPS time series). In the last part of the paper, we reveal a long–wavelength correlation between the pattern of coastal retreat along the Italian coasts and current GIA–induced sea level variations.

2 Methods

In this paper, present–day GIA–induced rates of sea level change ($\dot{S}$), vertical crustal deformation ($\dot{U}$), and geoid height variation ($\dot{N}$) are computed by means of the public–domain code SELEN (Spada and Stocchi, 2007), which solves the ”Sea **Level** Equation” (SLE) in the form of Farrell and Clark (1976) through the “pseudo–spectral” approach introduced by Mitrovica and Peltier (1991) and Mitrovica et al. (1994). SELEN assumes a radially stratified, incompressible Earth model and a linear Maxwell visco–elastic rheology. **Horizontal migration of shorelines and effects from Earth rotation instabilities are neglected**.

The SLE reads

$$S = \frac{\rho_i}{\gamma} G_s \otimes_i I + \frac{\rho_w}{\gamma} G_s \otimes_o S + S^E - \frac{\rho_i}{\gamma} \overline{G_s \otimes_i I} - \frac{\rho_w}{\gamma} \overline{G_s \otimes_o S}, \quad (1)$$

where I is ice sheets thickness variation, ρ_i and ρ_w are ice and water densities, respectively, $\otimes_i$ and $\otimes_o$ denote spatial and temporal convolutions over the ice– and ocean covered regions, γ is **[8/2] average gravity at the Earth's surface**, and the last two ocean–averaged terms ensure mass conservation. The sea level Green's function G_s accounts for mantle visco–elasticity through the load–deformation coefficients for vertical displacement (h) and incremental potential (k) (Farrell and Clark, 1976; Spada and Stocchi, 2006, 2007). The "eustatic term" S^E represents the (spatially uniform) sea level change for a rigid, non–gravitating Earth. The integral nature of the SLE (1) demands a recursive procedure (Spada and Stocchi, 2007). **[2/1] Once S is obtained from Equation 1, vertical deformation and change of geoid elevation are given by**

$$U = \rho_i G_u \otimes_i I + \rho_w G_u \otimes_o S, \quad (2)$$

and

$$N = \rho_i G_n \otimes_i I + \rho_w G_n \otimes_o S, \quad (3)$$

where G_u and G_n are appropriate Green's functions. The variables

S, U, and N obey the fundamental equation

$$S = N - U, \qquad (4)$$

which defines sea level variations (see e. g. Spada and Stocchi 2006).

Assuming ICE5G (Peltier, 2004) as reference ice chronology, we will solve the SLE for an Earth model characterized by a 65 km thick [**1/1**] **purely elastic lithosphere with PREM–averaged elastic parameters**, and upper and lower mantle viscosities (hence after η_{UM} and η_{LM}) of 3×10^{20} and 1×10^{22} Pa $\cdot$ s (Lambeck et al., 2004a), respectively. [**1/1**] **This viscosity profile (which will be referred to as RVKL) and lithospheric thickness have** been constrained by Italian Holocene relative sea level indicators (Lambeck et al., 2004a; Lambeck and Purcell, 2005; Antonioli et al., 2008). To assess more robustly how GIA contributes to ongoing sea level variations and vertical movements across the Italian region, in the following we will also consider three rheological models characterized by increasing contrast between upper and lower mantle viscosities (Tushingham and Peltier, 1991; Peltier, 2004; Lambeck and Purcell, 2005; Stocchi and Spada, 2007). RVM1 is characterized by a nearly uniform viscosity profile with $\eta_{UM} = 10^{21}$ Pa $\cdot$ s and $\eta_{LM} = 2\times10^{21}$ Pa $\cdot$ s, while RVM2 implies an increase of one order of magnitude between upper and lower mantle viscosity ($\eta_{UM} = 4 \times 10^{20}$ Pa $\cdot$ s and $\eta_{LM} = 4 \times 10^{21}$ Pa $\cdot$ s). For RVM3, $\eta_{UM} = 4 \times 10^{20}$ and $\eta_{LM} = 4 \times 10^{22}$ Pa $\cdot$ s. [**1/1**] **In this study we do not consider the effects of varying the thickness of the lithosphere, since from test computations (not shown here) we have verified that this parameter generally plays a minor role with respect to mantle viscosity. The role of lateral variations of lithospheric thickness in the study region cannot be fully addressed**

because of the spatial low resolution of current 3D GIA models (Spada et al., 2006).

3 Results

In Figures 1, 2, and 3 we show predicted present–day values of $\dot{S}$, $\dot{U}$, and $\dot{N}$, which obey the fundamental relationship **given by Equation 4**. In the bulk of the **central** Mediterranean, subsidence of the solid surface and of the geoid [. . .] mainly follow from the melt water load until the cessation of melting, which, according to model ICE5G, occurred 4000 yrs ago. Rates of subsidence increase southward and the resulting sea level change [. . .] reaches maximum rates between ~ 0.7 and 0.9 mm yr^{-1} in the bulk of the Tyrrhenian Sea (Sardinia), and South East of Italy, between Sicily and Greece (Ionian Sea). **The GIA–induced rate of sea level change shown in Figure 1 represent a significant fraction of the average rate of sea level rise (SLR) deduced by tide–gauges observations during the last century and mainly associated with the ongoing climatic variations (Douglas, 1991; Cazenave and Nerem, 2004)**.

The basic data that we will consider in this study are **shown in Figures 4 and 5**. **The first** illustrates rates of sea level change derived from annual means based on monthly values measured at the Italian PSMSL tide gauges network (data available from http://www.pol.ac.uk/). The French site of Marseille (Ma) and the Croatian tide gauge of Dubrovnik (Du) are also considered. While Marseille records the longest time series in the Mediterranean, covering the period from 1886 to **2004 with** a secular trend of $+1.2 \pm 0.1$ mm yr^{-1}, **[9/2] very close to that derived from the other two long records** of

Genova (Ge) and Trieste (Tr), Dubrovnik is important since it is representative of southern Adriatic and it is placed close to a continuous GPS station. Rates of GPS vertical deformation considered in **Figure 5** represent residual vertical velocities computed by means of a distributed processing approach and referred to the stable Corsica–Sardinia block, consistently with Table 4 and Figure 6b of Serpelloni et al. (2006).

In order to compare numerical results to **the** observed rates **of Figures 4 and 5**, we now compute $\dot{S}$ and $\dot{U}$ for ICE5G and the viscosity profiles of models RVM1, RVM2, RVM3 and RVKL. Figure 6a shows, as a function of latitude, observed rates of $\dot{S}$ and their error bars and predictions that follow transect "1" of Figure 1, connecting Genova (Ge) to Palermo (Pa), and passing through Sardinia (LM, Ca). Numbers in parentheses indicate the period of observation for each station. Though the 96 years long time–series of Genova is possibly the only one suitable for a reliable estimate of secular trend (Zerbini et al., 1996), the remaining Tyrrhenian tide gauges clearly indicate, from the end of nineteenth to the first decades of twentieth century, positive rates that vary between 1.0 and 1.6 mm yr^{-1}. The observed sea level rise **(SLR)** is found to be in agreement with predictions, which show on the whole a tendency to increase southward. The lowest values are obtained for RVM1 model (dotted), which predicts a sea level fall of -0.2 mm yr^{-1} in Genova. With increasing contrast between η_{UM} and η_{LM}, predicted curves are shifted towards larger values, as a consequence of the increased isostatic disequilibrium that is attained for such viscosity values. For models RVKL and RVM3, GIA approximately contributes to 30 and 40 % of observed **SLR**, respectively, thus leaving residuals that are smaller than the estimated global **SLR** of 1.0 to 2.0 mm yr^{-1} (Douglas, 1991; Douglas et al., 2000; Church et al., 2001), consistently with findings of

Tsimplis et al. (2005) **[12/2] and Marcos and Tsimplis (2007)**.

Predictions following **transect** "2" of Figure 1, which connects north eastern Adriatic (Tr, Ve) to Ionian sea (Ct) and crossing central Tyrrhenian (see frame b), are shown in Figure 6b. Tide gauges in Naples (Na) and Venezia (Ve) record rates in excess of 2.0 mm yr^{-1}, being significantly affected by local geological and anthropogenic factors (see e. g., Carminati and Di Donato 1999). Disagreement between predictions and observations from the remaining southern tide gauge stations, which record a sea level fall, may be attributed to local tectonic effects and to the short duration of sea level records. Figure 6c displays all the observed rates of sea level change of Figure 4 as function of record length. For time–series shorter or equal to $\sim$ 15 years, absolute values of observed rates largely exceed those expected from longest, secular records and show a significant scatter. **[10/2] According to Douglas (1992), tide gauges time series shorter than** 50 **years cannot be considered reliable indicators of sea level rise or acceleration**.

In Figure 7a we compare GPS vertical velocities displayed in Figure 5 with values predicted along **the three transects shown in** Figure 2. Observed vertical velocities are residuals computed by removing the average value of CAGL and AJAC (Serpelloni et al., 2006) from each vertical solution. In order to compare our results with observations we adopt the same reference frame and, for each viscosity profile, we remove the average value of CAGL and AJAC from our $\dot{U}$ predictions. Figure 7a shows observed vertical velocities as function of latitude compared to predicted values along a transect **"3"** connecting the **Swiss** station of ZIMM to the central Mediterranean (LAMP). Model predictions define a narrow band whose trend agrees with the cubic regression of data displayed by **the** grey spline. A satisfactory fit is also attained **for transect "4" running along the** Tyrrenhian coast of Italy, from ZIMM to NOT1, as shown in Figure 7b. From both Figure 7a and 7b it clearly appears that the long–wavelength pattern of vertical displacement in these regions is essentially driven by GIA. When a NW–SE trending direction is considered **(transect "5" in Figure 2)**, the agreement with GIA predictions is disrupted to indicate that present–day vertical displacements along the Appennines chain mainly results by local factors of geological and tectonic origin **(Figure 7c)**. Predicted and measured velocities clearly show opposite trends with varying latitude.

To better describe to what extent the spatial variability of current sea level change and vertical deformation in Italy is driven by GIA, in Figure 8 we compare $\dot{S}$ to $\dot{U}$ at the coastal sites of Cagliari, Genova, Civitavecchia and Dubrovnik (see Figure 4), where both tide gauges and GPS observations are available (for Civitavecchia, we consider the average vertical velocity of nearby stations INGR and ELBA **in** Figure 5) . Since observed and predicted vertical velocities are referred to the Corsica–Sardinia block (as described above), in order to compare $\dot{U}$ with $\dot{S}$, we refer also the observed and predicted rates of sea level change to the average value of Cagliari and La Maddalena. Since $\dot{N}$ shows little variability across the study region (see Figure 3), we expect that rates $\dot{S}$ and $\dot{U}$ would be negatively anti–correlated and consistent with observations if GIA is indeed the major driving process. From the results of Figure 8, the spatial variability of the referenced instrumental vertical velocities is in fact consistent with the GIA signal for all the viscosity profiles adopted, which define a narrow band within the errorbars. Values of $\dot{S}$ and $\dot{U}$ show a specular trend showing that despite different periods and uneven measurement time intervals, modern tide gauges and GPS records have been significantly affected by GIA and exhibit broadly consistent rates.

According to recent estimates, at least 70% of the world's beaches are experiencing a permanent retreat in response to extreme phenomena (e. g., storm waves) **exacerbated** by global sea level rise (Day, 2004). **[2/2] It is known that quantifying the relationship between SLR and beach erosion is not straightforward and that no universally accepted model of shoreline retreat has yet been developed (Cooper and Pilkey, 2004). The sensitivity of erosion to SLR can be tentatively studied using the Bruun rule (e. g. Bruun 1988), which predicts that the beach profile will shift landward by an amount $s/\tan\Theta$ where s is SLR and Θ is the profile slope angle. Although the Bruun rule omits many important variables (Cooper and Pilkey, 2004) and fails in specific areas (see e. g., Dickson et al. 2007), SLR is recognized as one of the main factors contributing to beach erosion, mainly operating by the increased destructive power of storms (Day, 2004).**

Since according to Figure 1 GIA determines a long–wavelength, non–uniform secular sea level rise that may reach an amplitude close to 1 mm yr^{-1}, it is reasonable to wonder whether GIA may indirectly influence current rates of erosion and beach retreat along the coastlines of Italy. To provide a tentative answer, we assume our reference model ICE5G(RVKL) and compute $\dot{S}$ along the coastlines of the Italian peninsula (see Figure 9a), Sicily (frame b) and Sardinia (c). Figure 9a shows that rates of sea level variation are everywhere in excess of 0.3 mm yr^{-1} and increase southward where rates of ~ 0.75 mm yr^{-1} are expected in the Calabria region (Ionian sea). According to the extensive review of GNRAC (2006), a similar trend is observed for the estimates of coastal erosion, which in Figure 9a (grey stepwise curve) is expressed in terms of length of retreating beaches (km) for the equal–length coastal **[11/2] traits based on the regional study shown in the Table of page 6 of GNRAC**.

Though estimates of regional coastal retreat are affected by large uncertainties, due in part to positive and negative feedbacks of man–made structures and human–driven imbalance of sediment supply (GNRAC, 2006), Figure 9a **[. . .]** shows that the trend of beach retreat **[2/2] broadly follows** that of the GIA–induced rate of sea level change, with a tendency to increase towards the south of the peninsula. Available data do not allow to discern spatial trends in Sicily and Sardinia (b and c), where 440 and 170 km of beaches are retreating, respectively, and relatively large rates of GIA–related **SLR** are expected. **[2/2] The non–linear relationship between SLR and beach erosion is manifest observing that while southern Calabria is presently uplifting in response to tectonic forces (Ferrantiet al., 2006), according to GNRAC (2006) the length of retreating beaches reaches its maximum in this region (c).**

4 Conclusions

Our analysis provides new estimates of current sea level variations and vertical land movements along the coasts of Italy in response to GIA, which, since the end of the last deglaciation, resulted in a generalized subsidence of the Italian peninsula. At specific sites, where tide gauges and continuous GPS stations are operating, this process provides a significant contribution to observed rates, which vary according to assumptions regarding the viscosity contrast across the 670 km depth seismic discontinuity. The fundamental equation that relates sea level changes with vertical displacements of the solid surface and of the geoid is broadly consistent with the rates of land movements and sea level changes inferred by modern instrumental data as well as by coastal archaeological observations reported by Lambeck et al. (2004b) and Antonioli et al. (2007). The latter provide relative sea level rates since historical times ($\sim 2000 - 2400$ years BP) of 0.8 mm yr^{-1} for Sardinia, 1.1 mm yr^{-1} for northern Adriatic (but for this area with an important tectonic contribution of 0.8 mm yr^{-1}) and 0.7 mm yr^{-1} for the peninsular coast of the Tyrrhenian sea. **According to our findings, GIA modulates the long–wavelength pattern of present–day sea level change along the coasts of Italy, but cannot explain vertical movements determined by GPS observations across the Apennines**.

Present day GIA–induced sea level variations are not spatially uniform. Rather, they systematically increase toward low latitudes reaching an amplitude of ~ 0.8 mm yr^{-1} along the coasts of the Ionian Sea and are superposed to the global signal associated with recent climatic forcing (Douglas, 1991), which may be assumed to be constant across the study region. For the first time, we have shown that at long–wavelengths this pattern is correlated with the length of retreating beaches for unit coastal traits (GNRAC, 2006), which supports the existence of tight (but complex) relationship between SLR and coastal erosion (Day, 2004). [. . .].

5 Acknowledgments

Work funded by MIUR (Ministero dell' Università, dell'Istruzione, e della Ricerca) by the PRIN2006 grant "Il ruolo del riaggiustamento isostatico postglaciale nelle variazioni del livello marino globale e mediterraneo: nuovi vincoli geofisici, geologici, ed archeologici". The numerical code employed in this study (SELEN, see http://flocolleoni.free.fr/SELEN.html) is freely available and can be requested to GS (email: giorgio.spada@gmail.com).

References

Antonioli, F., Anzidei, M., Lambeck, K., Auriemma, R., Gaddi, D., Furlani, S., Orrú, P., Solinas, E., Gaspari, A., Karinja, S., Kovaciĉ, V., Surace, L., 2007. Sea-level change during the Holocene in Sardinia and in the northeastern Adriatic (central Mediterranean Sea) from archaeological and geomorphological data. Quaternary Science Reviews 26, 24632486.

[15/2] **Antonioli F., Ferranti L., Fontana A., Amorosi A., M., Bondesan A., Braitenberg C., Dutton A., Fontolan G., Furlani S., Lambeck K., Mastronuzzi G., Monaco C., Spada G., Stocchi P., 2008**. Holocene relative sea-level changes and tectonic movements along the Italian coastline, Quaternary international, submitted.

[2/2] **Bruun, P., 1988. The Bruun rule of erosion by sea level rise: a discussion of large–scale two– and three–dimensional usages, Journal of Coastal Research 4, 627–648.**

Carminati, E, Di Donato, G., 1999. Separating natural and anthropogenic vartical movements in fast subsiding areas: the Po plain (N. Italy) case. Geophysical Research Letters 26, 2291–2294.

Cazenave, A., Nerem, R. S., 2004. Present-Day sea level change: observations and causes. Review of Geophysics 42, RG3001. doi : 10.1029/2003RG000139.

Church, J. A., J. M. Gregory, P. Huybrechts, M. Kuhn, K. Lambeck, M. T. Nhuan, D. Qin, and Woodworth, P. L., 2001. Changes in sea level, in Climate Change 2001: The Scientific Basis: Contribution of Working Group I to the Third Assessment Report of the Intergovernmental Panel on Climate Change, edited by J. T. Houghton et al., chap. 11, pp. 639–694, Cambridge Univ. Press, New York.

Clark, J. A., Lingle, C. S., 1979. Predicted Relative sealevel Changes (18.000

Years B.P. to present) Caused by **Late Glacial** Retreat of Antarctic Ice Sheet. Quaternary Research, 11, 279298.

[2/2] Cooper, J. A. G., Pilkey, O. H., 2004. Sea–level rise and shoreline retreat: time to abandon the Bruun rule, Global and Planetary Change 43, 157–171.

Day, C., 2004. Sea–level rise exacerbates coastal erosion, Physics Today, http://www.physicstoday.org/vol-57/iss-2/p24.html.

[2/2] Dickson, M. E., Walkden M. J. A., Hall, J. W., 2007. Systemic impacts of climate change on an eroding coastal region over the twenty–first century, Climatic Change 84, 141–166.

Douglas, B. C., 1991. Global sea level rise. Journal of Geophysical Research 96, 6981–6992.

Douglas, B. C., 1992. Global sea level acceleration. Journal of Geophysical Research 97, 12,699–12,706.

Douglas, B. C., Kearney, M. S., Leatherman, S. P., 2000. Sea Level Rise: History and Consequences. Academic Press, 232 pp.

Farrell, W. E., Clark, J. A., 1976. On postglacial sea level. Geophysical Journal of the Royal Astronomical Society 46, 647–667.

[2/2] Ferranti, L., Antonioli, F., Mauz, B., Amorosi, A., Dai Pra, G., Mastronuzzi, G., Monaco, C., Orrù, P., Pappalardo, M., Radtke, U., Renda, P., Romano, P., Sansò, P., Verrubbi, V., 2006. Markers of the last interglacial sea-level high stand along the coast of Italy: Tectonic implications, Quaternary International, 145–146, 30–54.

GNRAC (Gruppo Nazionale per la Ricerca sull'Ambiente Costiero), 2006. Studi Costieri 10, 174 pp.

Lambeck, K., Johnston, P., 1995. Land subsidence and sealevel change: contributions from the melting of the last great ice sheets and the isostatic adjustment of the Earth. In: Barends, F. B. J. et al. (Eds.), Land Subsidence. Balkema, Rotterdam, pp. 3–18.

Lambeck, K., Antonioli, F., Purcell, A., Silenzi, S., 2004a. Sea level change along the Italian coast from the past 10,000 yr. Quaternary Sciences Reviews 23, 1567–1598.

Lambeck, K., Anzidei, M., Antonioli, F., Benini, A., Esposito, A., 2004b. Sea level in Roman time in the Central Mediterranean and implications for recent change. Earth and Planetary Science Letters 224, **563–575.**

Lambeck, K., Purcell, A., 2005. Sea–level change in the Mediterranean Sea since th LGM: model predictions for tectonically stable areas, Quat. Sciences Reviews 24, 1969–1988.

Marcos, M., Tsimplis, M. N., 2007. Forcing of coastal sea level rise patterns in the North Atlantic and the Mediterranean Sea. Geophysical Research Letters 34. doi:10.1029/2007GL030641.

Mitrovica, J. X., Peltier, W. R., 1991. On post–glacial geoid subsidence over the equatorial ocean. Journal of Geophysical Research 96, 20,053–20,071.

Mitrovica, J. X., Davis, J. L., Shapiro, I. I., 1994. A spectral formalism for computing three–dimensional deformations due to surface loads. Journal of Geophysical Research 99, 7057–7073.

Peltier, W. R., 2004. Global Glacial Isostasy and the Surface of the Ice-Age Earth: The ICE-5G(VM2) model and GRACE. Annual Reviews of Earth and Planetary Sciences 32, 111-149.

Pirazzoli, P. A., 1991. World atlas of Holocene sea–level changes, Elsevier, Amsterdam, 300 pp.

Pirazzoli, P. A., 2005. A review of possible eustatic, isostatic, and tectonic contributions in eight late–Holocene relative sea–level histories from the

Mediterranean area, Quaternary Sciences Reviews 24, 1989–2001.

Serpelloni, E., Casula, G., Galvani, A., Anzidei, M., Baldi, P., 2006. s Data analysis of permanent GPS networks in Italy and surrounding regions: Application of a distributed processing approach. Annals of Geophysics, 49.

Spada, G., Antonioli, A., Cianetti, S., Giunchi, C., 2006. Glacial isostatic adjustment and relative sea-level changes: the role of lithospheric and upper mantle heterogeneities in a 3-D spherical Earth. Geophysical Journal International 165. doi: 10.1111/j.1365- 246X.2006.02969.x

Spada G., Stocchi, P., 2006. The Sea Level Equation, Theory and Numerical Examples. Aracne, Roma, 96 pp.

Spada, G., Stocchi, P., 2007. SELEN: a Fortran 90 program for solving the "Sea Level Equation". Computers and Geosciences 33. doi: 10.1016/j.cageo.2006.08.006.

[**13/2, 14/2**] Stocchi, P., Spada, G., Cianetti, S., 2005. Isostatic rebound following the Alpine deglaciation: impact on the sealevel variations and vertical movements in the Mediterranean region. Geophysical Journal International 162. doi: 10.1111/j.1365-246X.2005.02653.x.

Stocchi, P., Spada, G., 2007. Glacio and hydro–isostasy in the Mediterranean Sea: Clark's zones and role of remote ice sheets. Annals of Geophysics, 50 (6), in press.

Tsimplis, M. N., Álvarez–Fanjul, E., Gomis, D., Fenoglio–Marc, L., Pérez, B., 2005. Mediterranean Sea level trends: Atmospheric pressure and wind contribution. Geophysical Research Letters 32. doi:10.1029/2005GL023867.

Tushingham, A. M., Peltier, W. R., 1991. Ice-3G: a new global model of late Pleistocene deglaciation based upon geophysical prediction of post–glacial sea level change. Journal of Geophysical Research 96, 4497–4523.

Zerbini S., Plag H.-P., Baker T., Becker M., Billiris H., Burki B.,

Kahle H.-G., Marson I., Pezzoli L., Richter B., Romagnoli C., Sztobryn M., Tomasi P., Tsimplis M., Veis G., Verrone G., 1996. Sea level in the Mediterranean: a first step towards separating crustal movements and absolute sea–level variations. Global and Planetary Change 14, 1–48.

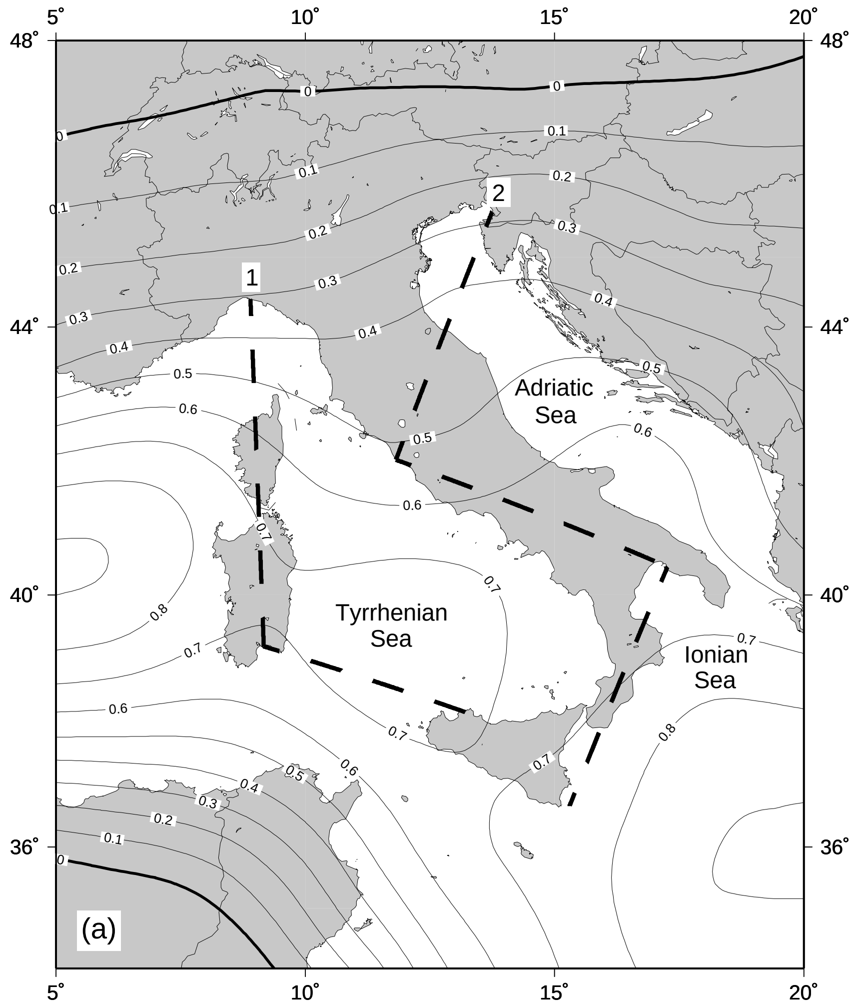

Fig. 1. [**4/2**] **Predicted rate (mm yr^{-1}) of present–day sea level change $\dot{S}$ according to our reference model ICE5G(RVKL). Here and in the following, the maximum harmonic degree is $L_{max} = 96$ and the spatial resolution of the integration grid is $R = 28$ (this corresponds to a spatial discretization by 30252 pixels on the surface of the sphere, see Spada and Stocchi 2007). Dashed lines show transects "1" and "2" considered in Figure 6.**

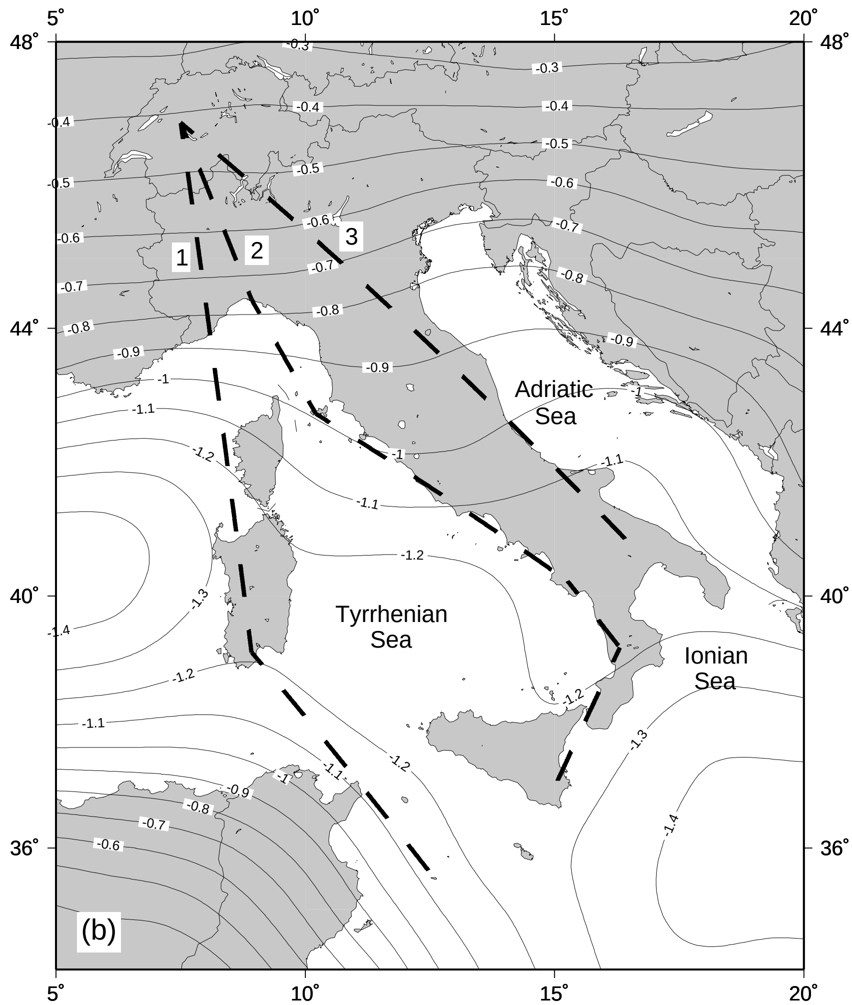

Fig. 2. [4/2] **Rate of present–day vertical deformation (mm yr^{-1}) of the solid surface of the Earth $\dot{U}$, according to the same model of Figure 1. Dashed lines show the transects "3", "4", and "5" discussed in the text and considered in Figure 7** .

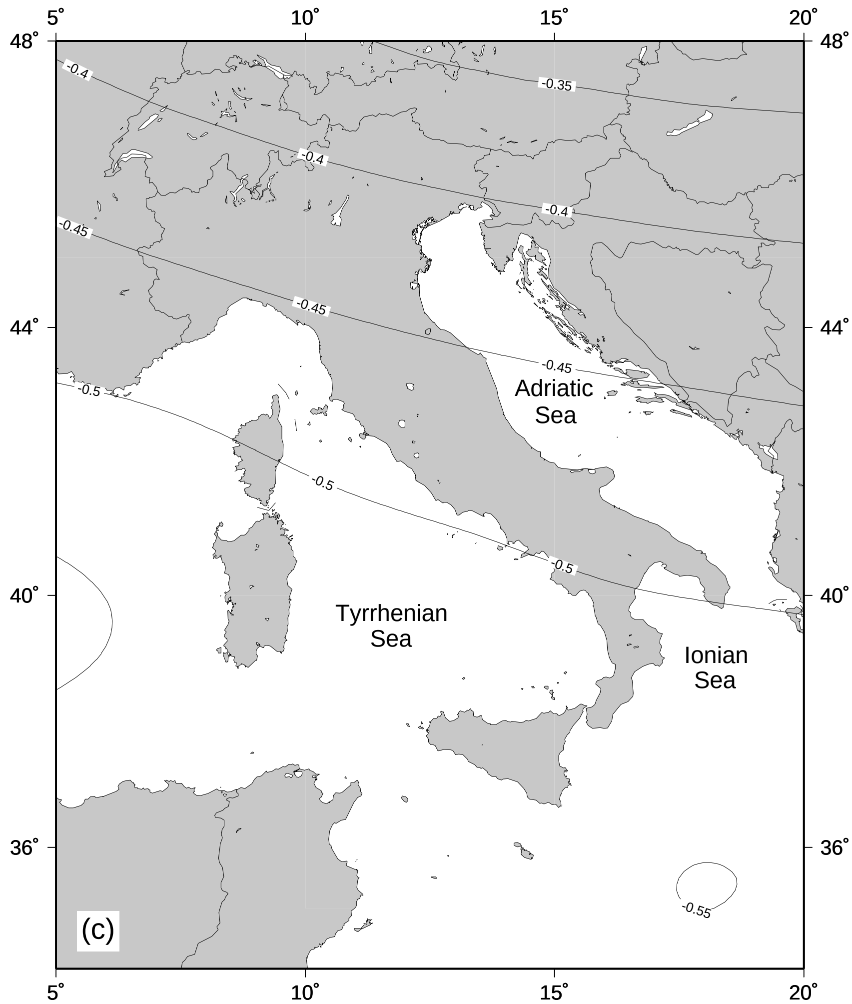

Fig. 3. **Present–day rate of change of geoid height $\dot{N}$ (mm yr^{-1}), according to the same model of Figure 1. $\dot{N}$ is given by $\dot{S}+\dot{U}$ (see Equation 4), where $\dot{S}$ and $\dot{U}$ are shown in Figures 1 and 2, respectively.**

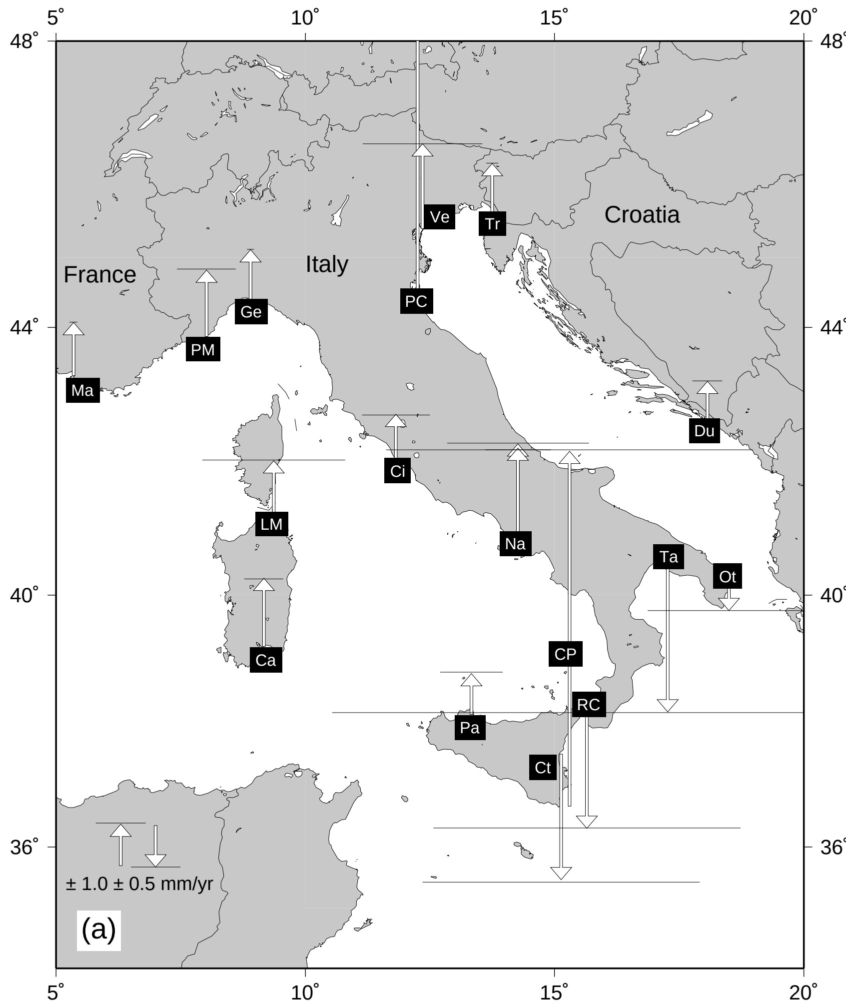

Fig. 4. **Measured rates of sea level change at tide gauges pertaining to the PSMSL tide gauges network (a). [5/2] PSMSL stations abbreviations refer to the italian stations contained in the PSMSL table of mean sea level trends (see page http://www.pol.ac.uk/psmsl/datainfo/rlr.trends), with the addition of Marseille (Ma) and Dubrovnik (Du).**

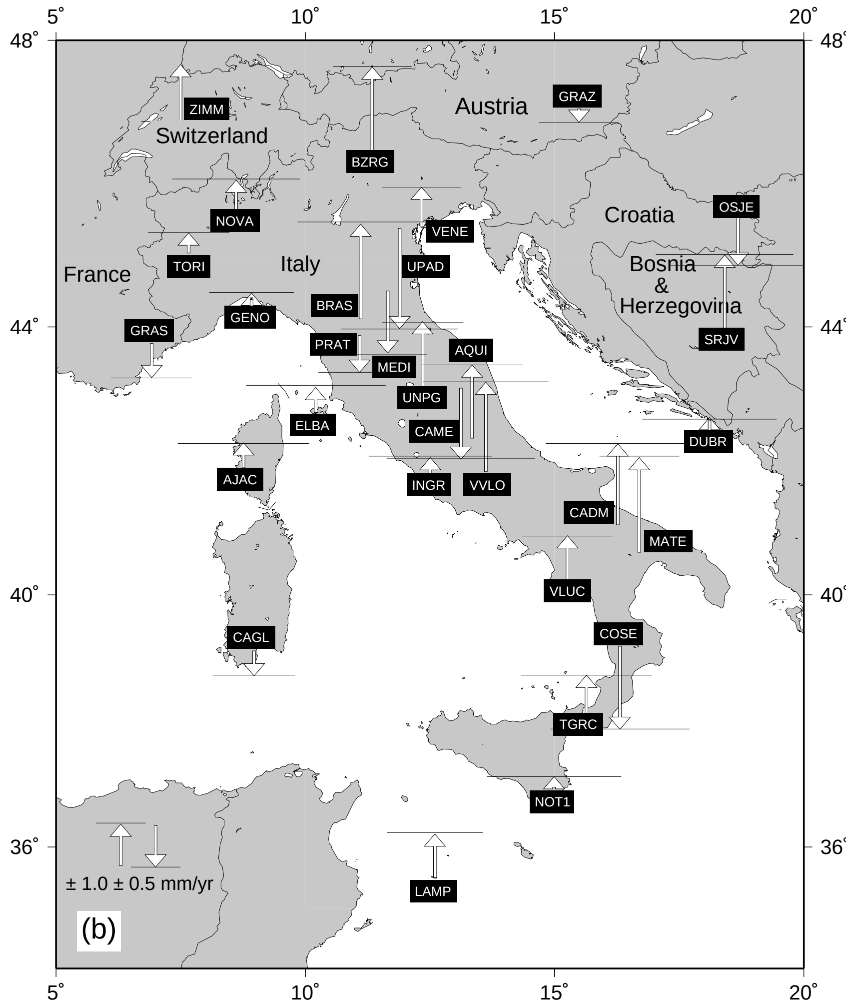

Fig. 5. **Vertical velocity solutions referred to the stable Corsica–Sardinia block from continuous GPS stations of Table 4 in Serpelloni et al. (2006).**

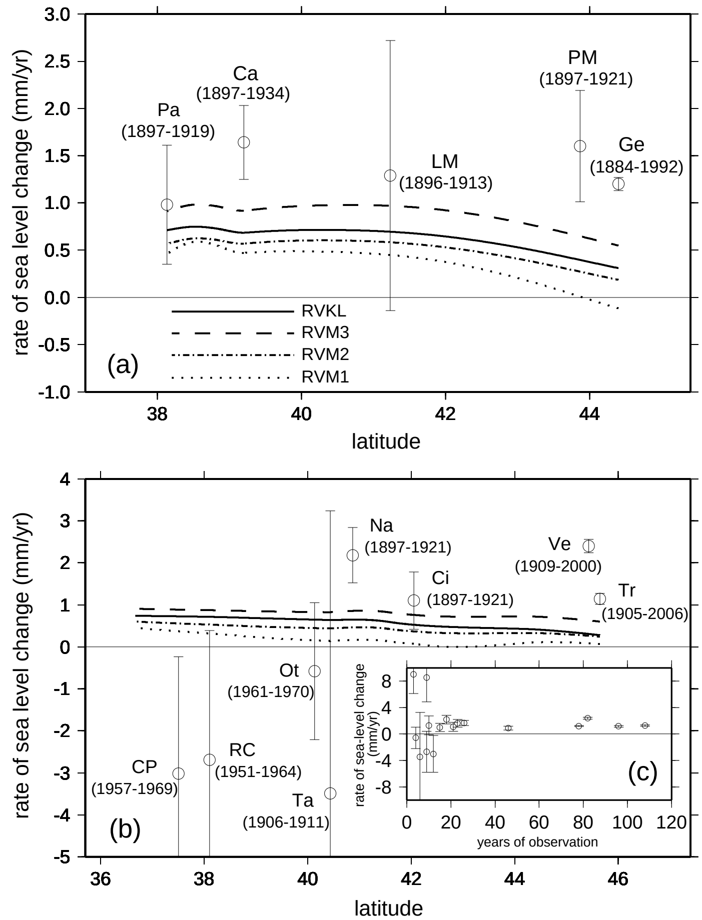

Fig. 6. Frames (a) and (b): observed and predicted $\dot{S}$ along the two transects shown in Figure 1, respectively. Stations abbreviations as in Figure 4. **[5/2] Rates and their uncertainties are computed using the PSMSL annual 'RLR' (Revised Local Reference) dataset (see http://www.pol.ac.uk/psmsl/) by straightforward least squares. The time interval used for rate calculation is shown next to each datum**. **Frame** (c) shows the recorded trend of sea level change as a function of the years of observations **for all tide gauges considered.**

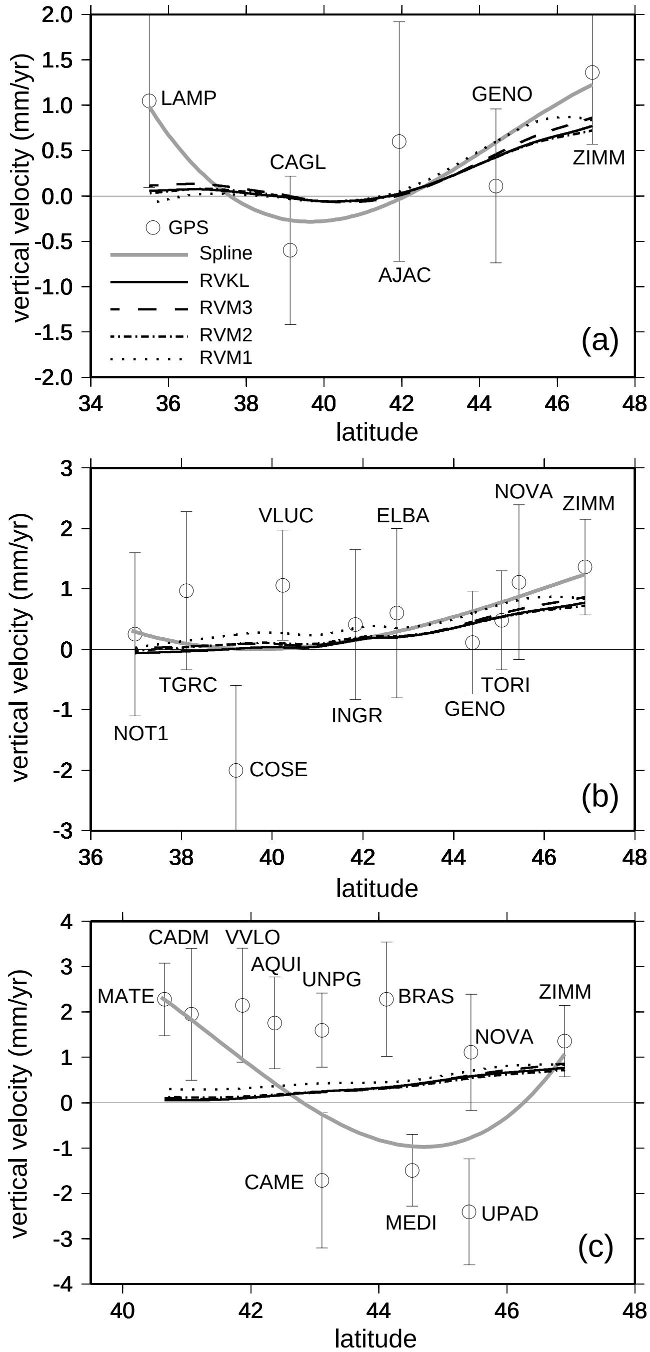

Fig. 7. Observed and predicted $\dot{U}$ along GPS stations placed along the three transects shown in Figure 2. **The grey curve is a cubic regression spline of observed $\dot{U}$ values derived from geodetic data.**

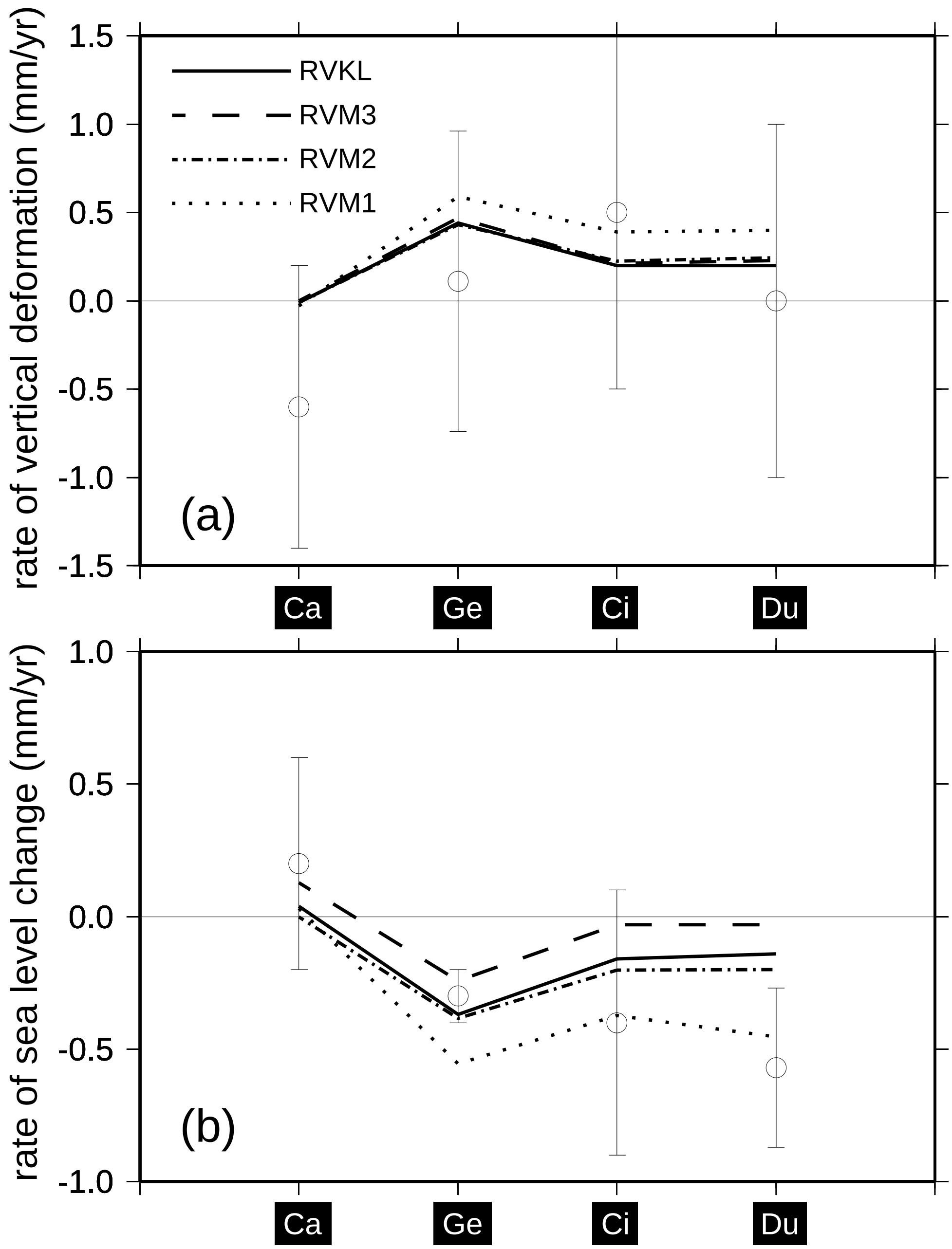

Fig. 8. [**6/2**] **Predicted** $\dot{U}$ **(a) and** $\dot{S}$ **(b) at the sites of Cagliari (Ca), Genova (Ge), Civitavecchia (Ci), and Dubrovnik (Du), compared to GPS (a) and tide–gauge observations (b)** for model RVKL and the other three **mantle viscosity** profiles discussed in the text.

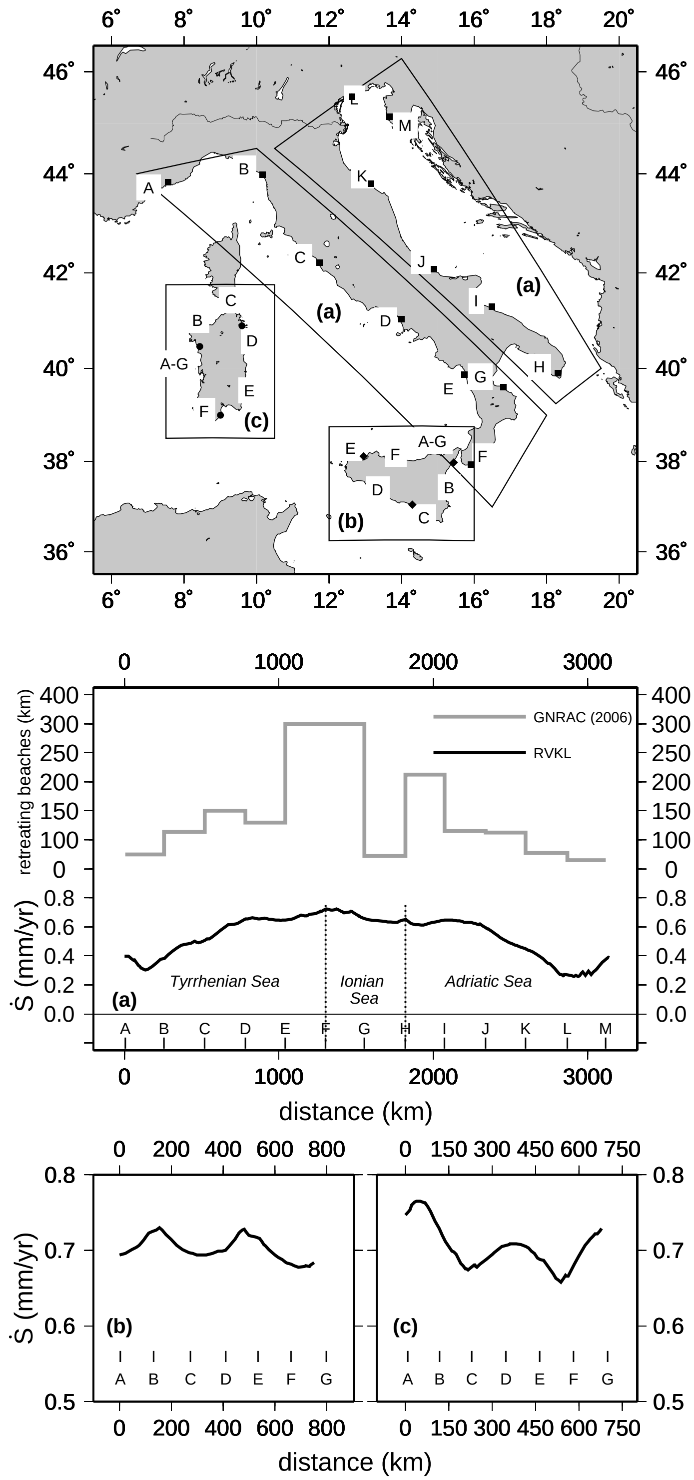

Fig. 9. Predicted $\dot{S}$ for ICE5G(RVKL) and estimated length of retreating beaches according to GNRAC (2006), relative to the Italian peninsula (a), Sicily (b), and Sardinia (c).